Engineering a Nanostructured Nucleolin-Binding Peptide for Intracellular Drug Delivery in Triple-Negative Breast Cancer Stem Cells

Mireia Pesarrodona[∞#‡], Laura Sánchez-García[#∞ƒ‡], Joaquin Seras-Franzoso[¥], Alejandro Sánchez-Chardi[§], Ricardo Baltà-Foix[¥†], Patricia Cámara-Sánchez[#¥∂], Petra Gener[#¥], José Juan Jara[#+], Daniel Pulido[#+Δ], Naroa Serna[∞#], Simó Schwartz Jr[#¥], Miriam Royo[#+Δ], Antonio Villaverde[∞#ƒ], Ibane Abasolo[#¥∂]*, Esther Vázquez[∞†#ƒ].*

∞ Institut de Biotecnologia i de Biomedicina, Universitat Autònoma de Barcelona, Bellaterra, 08193 Barcelona, Spain

CIBER de Bioingeniería, Biomateriales y Nanomedicina (CIBER-BBN), C/ Monforte de Lemos 3-5, 28029 Madrid, Spain

ƒ Departament de Genètica i de Microbiologia, Universitat Autònoma de Barcelona, Bellaterra, 08193 Barcelona, Spain

¥ Drug Delivery & Targeting CIBBIM-Nanomedicine, Vall d'Hebron Institut de Recerca (VHIR), Universitat Autònoma de Barcelona, 08035 Barcelona, Spain

§ Departament de Biologia Evolut iva, Ecologia i Ciències Ambientals, Facultat de Biologia, Universitat de Barcelona, 08028 Barcelona, Spain

∂ Functional Validation & Preclinical Research, CIBBIM-Nanomedicine, Vall d'Hebron Institut de Recerca (VHIR), Universitat Autònoma de Barcelona, 08035 Barcelona, Spain

+ Combinatorial Chemistry Unit, Barcelona Science Park, Universitat de Barcelona, 08028 Barcelona, Spain

Δ Multivalent Systems for Nanomedicine, Institute for Advanced Chemistry of Catalonia (IQAC-CSIC), Barcelona, 08034, Spain

ABSTRACT

Five peptide ligands of four different cell surface receptors (nucleolin, CXCR1 CMKLR1 and CD44v6) have been evaluated as targeting moieties for triple-negative human breast cancers. Among them, the peptide F3, derived from phage display, promotes the fast and efficient internalization of a genetically fused GFP inside MDA-MB-231 cancer stem cells, in a specific receptor-dependent fashion. The further engineering of this protein into the modular construct F3-RK-GFP-H6 and the subsequent construct F3-RK-PE24-H6, resulted in self-assembling polypeptides that organize as discrete and regular nanoparticles. These materials, of 15-20 nm in size, show enhanced nucleolin-dependent cell *penetrability*. We show that the F3-RK-PE24-H6, based on the *Pseudomonas aeruginosa* exotoxin A (PE24) as a core functional domain, is highly cytotoxic over target cells. The combination of F3, the cationic peptide (RK)n, and the toxin domain PE24 in such unusual presentation appears as a promising approach to cell-targeted drug carriers in breast cancers and address selective drug delivery in otherwise difficult-to-treat triple-negative breast cancers.

KEYWORDS

Self-assembling polypeptides; targeting; nucleolin; triple negative breast cancer; cancer stem cells

1. Introduction

Cancer is one of the leading causes of death in developed countries, with breast carcinoma being the most frequently diagnosed cancer and the leading cause of cancer death in females worldwide.[1] Among one million cases of breast cancer diagnosed each year, approximately 15 % are characterized as triple-negative (triple negative breast cancer, TNBC), lacking the expression of estrogen receptor (ER), progesterone receptor (PgR) and HER2/neu receptor.[2] Absence of effective therapies, younger age of onset, and early metastatic spread have contributed to the poor prognoses and outcomes associated with this malignancy. Unlike patients with ER/PgR+ and/or HER2 overexpressing disease, with positive responses to endocrine or HER2-targeted therapies, systemic treatment options for TNBC are limited to the cytotoxic chemotherapy. Anthracyclines and taxanes are the most active and widely used chemotherapeutic agents for TNBC, but they have important drawbacks. Combination of antracyclines and taxanes deal with serious cytotoxic side-effects [3] and more importantly, a subset of TNBC patients will present early, aggressive metastatic relapse.[2] The increased use of these chemotherapeutics at an early stage of disease often renders tumors resistant to these drugs and, by the time the disease recurs, thereby reducing the number of treatment options for metastatic disease. [4,5]

Evidences that breast cancer maintenance, resistance to therapy and metastatic disease are sustained by cancer stem cells (CSC) are recently accumulating.[6] In breast cancer, these cells correspond to a small fraction of cells within the tumor that express stem cell markers (CD44+/CD24-/low/lin-) and have the ability to grow as spheres and differentiate into defined progenies, and initiate and sustain tumor growth *in vivo*.[7] According to the "cancer stem cell hypothesis", cancers originate from the malignant transformation of an adult stem cell, through the deregulation of the normally tightly regulated self-renewal program. This leads to the clonal

expansion of stem/progenitor cells that undergo further genetic or epigenetic alterations to become fully transformed. As a consequence, tumors contain a cellular compartment of CSCs that retain the capacity of repopulating the tumor while being insensitive to conventional anticancer therapies, antimitotic agents or radiation.[8] Interestingly, TNBC have a basal-like gene signature, and basal-like breast cancers are enriched in CSC. In this regard, new therapies against TNBC should compile two requirements: (i) reduce the toxicity seen in combination therapies and most importantly, (ii) specifically target and eliminate CSCs. In this scenario, emerging nanomedical approaches in oncology [9,10] could be useful to improve drug therapeutic indexes based on active receptor-based targeting to CSC. Most conveniently, the targeted drug itself should be desirably organized as a nanoscale structure, to avoid the use of nanoscale carriers with potential side toxicities.[11] Proteins are specially versatile and appropriate to construct nanoscale drugs and functional materials for targeted cancer therapies based on self-assembly peptides or protein domains. [12,13]

Following this concept, we first explored ligands of cell surface proteins overexpressed in populations of TNBC cells, namely nucleolin,[14,15] CXCR1,[16,17] CMKLR1 or chemerin receptor [18] and CD44v6,[19,20] still unwell examined as potential targets for drug delivery. In this context, we wondered if peptide ligands of these receptors could serve as a basis for the development of protein-based carriers for intracellular delivery in cancer cells.

2. Experimental section

Peptide synthesis

Carboxyfluoresceinated derivatives from hv6pep, pw14, sCH9 and p17 peptide ligands were synthesized manually using the 2-Chlorotrityl Chloride resin following a Fmoc/tBu synthesis

strategy. The peptide elongation was carried out using diisopropylcarbodiimide (DIC) and HOBt·H2O as coupling reagents and Fmoc elimination was performed by treatments with piperidine:DMF (2:8, v/v). Once the peptide sequence elongation was accomplished, each peptidyl-resin was split in two parts. One part was derivatized with carboxyfluorescein (CF) directly linked to the N-terminus of the peptide ligand sequence. To the other part, Fmoc-6-aminohexanoic acid spacer was introduced onto the N-terminus of the peptide sequence, which was subsequently modified with CF after the previous elimination of the Fmoc protecting group. Peptides were cleaved from the resin by an acidolysis treatment with trifluoroacetic acid (TFA-H2O-TIS, 95: 2.5: 2.5).

Carboxyfluoresceinated version of peptide ligand F3 was synthesized by a convergent strategy using two protected peptide fragments (Fragment F3A (1-15) and fragment F3B (16-30)). Both peptide fragments were synthesized on a Liberty Lite microwave peptide synthesizer (CEM corporation) using a HMPB-ChemMatrix resin previously functionalized with the C-terminal amino acid, which was incorporated manually using the Fmoc-aa, DIC and 4-dimethylaminopyridine (DMAP). Both fragment peptides were elongated using a Fmoc/tBu synthesis strategy. The Fmoc elimination was performed with 10% piperazine (w/v) in NMP-EtOH (9:1, v/v) mixture, DIC and Oxyma Pure were used as coupling reagents and dimethylformamide (DMF) as solvent. Once the peptide elongation was finished, CF was incorporated onto the F3A peptidyl-resin and both peptidyl-resins (CF-F3A and F3B) were cleaved by an acidolysis treatment with TFA:DCM (2:98, v/v). Then, peptide fragment F3B was coupled to NH2-Lys(Boc)-OtBu in solution, generating the fully protected peptide fragment F3C (15-31). The Fmoc protecting group of the N-terminus residue of the F3C fragment was eliminated by treatment with diisopropylethylamine in dichloromethane (DIEA in DCM). Later,

peptide fragment CF-F3A was reacted with peptide fragment F3C using PyBOP: DIEA as coupling reagents, rendering the protected CF-F3 peptide. Finally, CF-F3 peptide was obtained after an acidolysis treatment with TFA (TFA-H2O-TIS, 95: 2.5: 2.5) to eliminate tBu based side chain protecting groups, and a precipitation in diethyl ether.

All carboxyfluoresceinated peptide ligands were analyzed by HPLC and HPLC-MS and purified by semipreparative HPLC-MS. Purity of final peptides was ≥90%.

Protein expression and production

Ligand-presenting GFP-H6 constructs were expressed as recombinant proteins in *Escherichia coli* BL21 under IPTG-induced pET22b expression vector. A culture of *E. coli* cells in LB media was induced upon addition of 1 mM IPTG when OD reached 0.5 and was further cultivated overnight at 20 ºC. Cells were centrifuged at 5,000 *g* for 15'. Pellet was washed with PBS and then resuspended in lysis buffer (20 mM TrisHCl, 500 mM NaCl, 10 mM Imidazole; pH 8.0) with Complete protease inhibitor cocktail (Roche).

Purification of the His-tagged constructs was performed by Nickel affinity chromatography. Cell suspension was lysated by French Press at 1,200 psi and lysate was centrifuged at 15,000 *g* for 45'. Supernatant was filtered and injected to a HiTrap Chelating HP column using an AKTA system. Protein was eluted applying an imidazole gradient to 500 mM and dialyzed against carbonate buffer (166 mM $NaCO_3H$; pH 7.4). Protein purity was analyzed by SDS-PAGE Coomassie Brilliant Blue staining and Western blot incubating with anti-His antibody (Santa Cruz Biotechnology). Protein concentration was determined by Bradford's assay.

Dynamic light scattering

Protein and nanoparticles size distribution was by dynamic light scattering at 633 nm (Zetasizer Nano ZS, Malvern Instruments).

Electron microscopy

Ultrastructural characterization of nanoparticle morphometry (size and shape) articles was determined at nearly native state with field emission scanning electron microscopy (FESEM). Drops of 3 µl of F3-RK-GFP-H6 (C), and F3-RK-PE24-H6 (CS) samples diluted at 0.3 mg/ml in their respective buffers were directly deposited on silicon wafers (Ted Pella Inc.) for 30 s. Excess of liquid was blotted with Whatman filter paper number 1 (GE Healthcare), air dried for few min and immediately observed without coating with a FESEM Zeiss Merlin (Zeiss) operating at 1 kV and equipped with a high resolution *in-lens* secondary electron detector. Representative images of a general field and nanoparticle detail were captured at three high magnifications (from 150,000x, 250,000x and 400,000x).

Cell culture and flow cytometry

MDA-MB-231 breast cancer cell line was routenely maintained in RPMI 1640 supplemented with 10 % fetal bovine serum (FBS) and 6 mM GlutaMAX (Invitrogen). Breast cancer cell lines naturally contain CSC.[21] To facilitate the enrichment of CSC within the MDA-MB-231 cell line, mammosphere were cultured as previously described [22] in low attachment plates (Corning) in serum-free RPMI 1640 supplemented with 60 mg/mL glucose, 10 µL/mL L-glutamine, 10 µL/mL antibiotic-antimitotic mixture (Life Technologies), 0.01 µg/mL FGFb (Thermo Fisher Scientific), and 4 µg/mL heparin, 2 mg/mL BSA, 0.02 µg/mL EGF, 10 µg/mL putrescin, 0.1

mg/mL apo-transferrin, 25 µg/mL insulin, 30 µM selenium, and 20 µM progesterone (all from Sigma).

Flow cytometry

Peptide internalization assessment was performed in MDA-MB-231 cells grown in attachment or non-attachment conditions after 4 h of incubation of 1.5 µM peptide (10,000 and 1,000 cells/well, respectively in corresponding 96 well-plates). On the other hand, for analyzing the entry of protein constructs, cells were seeded on 24-well plates at 80,000 cells/well and incubated in presence of OptiPRO SFM (serum-free medium) and L-glutamine for 24 h. Competition experiments with protein constructs were performed adding lactoferrin (Sigma-Aldrich) at 1:3 and 1:10 ratio 1 h before protein incubation, and maintained afterwards. After the incubation, cells were collected using a harsh protocol that removes all the protein attached in the cellular membrane adding 1 mg/ml of Trypsin-EDTA (Gibco) for 15 min at 37 ºC. Finally, samples were analyzed using a FACS-Canto or LSR Fortessa flow cytometer (Becton Dickinson). Experiments were performed in duplicate.

Cell viability

The cytotoxicity of F3-RK-PE24-H6 protein was assessed using the CellTiter-Glo® Luminescent Cell Viability Assay (Promega). MDA-MB-231 cells were cultured on 96-well opaque plates at 2,500 cells/well for 24 h at 37 ºC until reaching 70 % confluence. Proteins were incubated at 0.1, 1 and 3 µM for 24 and 48 h. Cell death specificity was tested at 48 h adding the competitor lactoferrin (Sigma) at 1:3 ratio 1 h prior to protein incubation (0.1 µM) and maintained afterwards. Samples luminescence was measured with a conventional luminometer, Victor3 (Perkin Elmer). Experiments were performed in triplicate.

Statistical analysis

Pairwise comparisons between groups were determined by Tukey's test. Divergences between groups were considered significant at $p < 0.05$ and relevant significances were indicated as * for $0.01 < p < 0.05$ and ** for $p < 0.01$ in the figures. Quantitative data were expressed as mean ± standard error of the mean (SEM). Past3 software was employed to perform statistical analysis.

3. Results and discussion

Five different peptides were selected to target nucleolin, CXCR1, CMKLR1 and CD44v6 receptors based on previous findings in the literature (Figure 1A). In order to test the selectivity of these peptides to CSC, they were synthesized and linked to 5(6)-carboxyfluorescein (CF), with or without the aminohexanoic (Ahx) linker (Supplementary Figure 1A) and incubated with MDA-MB-231 cells (ATCC® HTB-26™), in normal cell culture conditions, in monolayers and with complete media, or in low attachment conditions, with a specific media. MDA-MB-231 is a poorly differentiated triple-negative breast cancer cell line, ER, PgR and E-cadherin negative, commonly used as *in vitro* model for triple-negative breast cancer.[23] MDA-MB-231 cells growing in low attachment conditions form mammospheres, which are naturally enriched in CSC. Thus, we measured the internalization of peptides in attachment and low-attachment conditions (Figure 1B). All peptides except sCH9 showed a better internalization in low attachment conditions. Moreover, these assays revealed that F3 and P17 were the peptides with the highest internalization in CSC enriched cultures (Figure 1B). Based in these results, sCH9 was discarded for future developments.

A

Target	Peptide ligand	References	Sequence
CD44v6	hv6pep	[20, 24]	KEQWFGNRWHEGYR
CXCR1	pw14	[16, 21,25,26]	QCIKTYSKPFHPKF
CXCR1	p17	[16, 21, 25, 31, 32]	SGGELDRWEKIRLRPGGKKK
CMKLR1	sCH9	[18, 27, 28]	YChaPGMYAFS
Nucleolin	F3	[14, 29]	KDEPQRRSARLSAKPAPPKPEPKPKKA PAKK

B

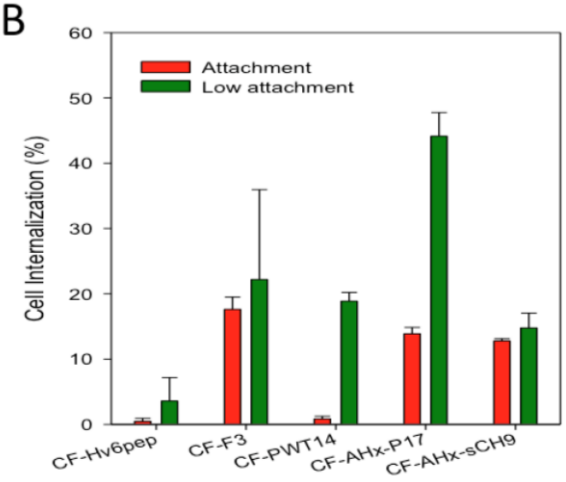

Figure 1. Evaluation of the internalization potential of peptide ligands selected for targeting specific CSC receptors. A) Selected peptide ligands for CD44v6,[20,24] CXCR1,[16,21,25,26] CMKLR1 [18,27,28] and nucleolin [14,29] receptors which are overexpressed in CSC. B) Internalization of chemically synthesized peptide ligands conjugated with CF. Cell penetrability was evaluated by flow cytometry in MDA-MB-231 cells grown in attachment or low-attachment conditions after 4 h incubation. Data represent mean ± SEM of a representative experiment.

In a step further, we designed larger protein constructs containing the selected targeting peptides with good internalization profiles. In detail, F3 peptide, identified by phage display techniques due to its high affinity for nucleolin,[29,30] the CXCL8-derivative pwt14 [26] and HIV p17

matrix protein [31,32] that interact with CXCR1, and hv6pep that binds the CD44v6.[24] Among them, F3 had been previously assayed in form of fusion protein with gelonin, a ribosome-inactivating protein,[33] and the F3 selective binding to nucleolin largely determined,[29,34,35] what represents a solid potential as a tumor-homing peptide in anti-cancer therapies.[14,34–37] Therefore, four fusion proteins were then constructed with each of those peptides at the amino terminus, followed by a core protein (GFP) and a carboxy terminal hexa-histidine (H6) peptide (Figure 2A). GFP provided a simple marker to trace cell internalization and H6, apart from offering a tool for single-step purification from cell extracts of producing recombinant bacteria, was expected to enhance endosomal escape upon uptake.[38] The recombinant genes were highly expressed in *Escherichia coli* and modular proteins synthesized and purified as stable, full-length forms (Supplementary Figure 2) ranging between 5 to 7 nm size (Figure 2B). These proteins were added to the culture media of regular MDA-MB-231 cells to test their internalization capacities vs. the GFP-H6 control construct. All tested proteins were efficiently internalized in a dose-dependent fashion (Figure 2C) reaching values above 40% of positive cells after 24 h incubation at 3 μM. The use of protein constructs indeed facilitated the cell entry compared to the single ligand peptides, whose cell uptake was below 20% even at long incubation times. Among all protein constructs, those binding nucleolin (F3-GFP-H6) and CXCR1 (pwt14-GFP-H6 and p17-GFP-H6) were the more efficient in terms of cell internalization, reaching higher percentage of MDA-MB-231 internalized cells. F3-construct, at 3 μM, showed 10-fold higher cellular uptake than the GFP-H6 control, and 1.4-fold higher uptake than the next protein construct with the best internalization profile (pw14-GFP-H6). Even at lower concentrations (1 μM), the number of cells incorporating F3-GFP-H6 doubled positive cells for pw14-GFP-H6 or other receptor targeted constructs. Therefore, the F3 was observed as the best candidate to

promote molecular binding and internalization of protein constructs in this cell line, and it was consequently selected for further studies.

A

Protein	MW (kDa)	mg/L	Ligand charged AA	
			+	-
hv6pep-GFP-H6	30.1	58	3	2
F3-GFP-H6	31.6	115	11	3
pwt14-GFP-H6	29.9	120	3	0
p17-GFP-H6	30.5	67	7	3

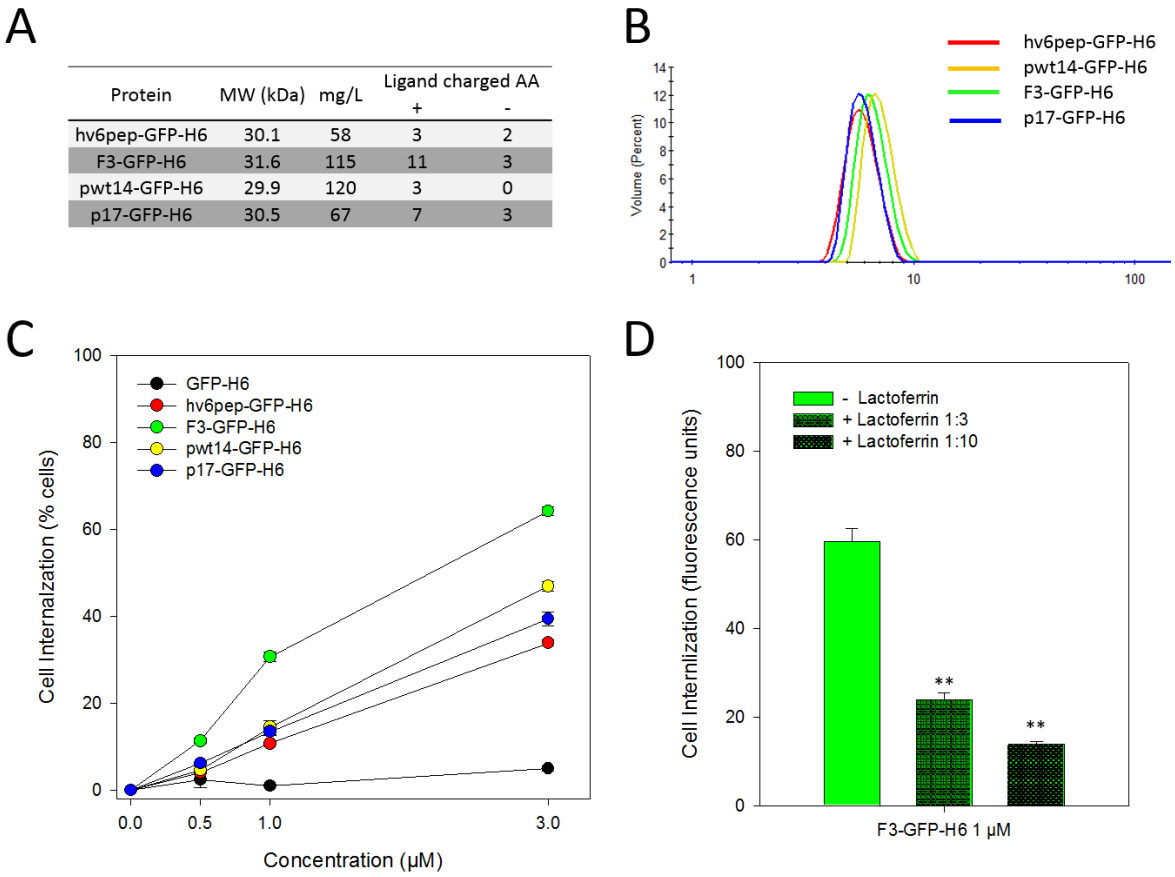

Figure 2. Physicochemical characterization and internalization evaluation of peptide-presenting GFP modular proteins. A) Theoretical molecular weight and recombinant production yield (mg protein/L of culture) of modular proteins. Number of negative and positive charged amino acids (AA) on peptide ligands. B) Hydrodynamic size of modular proteins by DLS ranging from 5 to 7 nm diameter. C) Concentration-dependent internalization by flow cytometry of peptide-presenting modular proteins after 24 h incubation in MDA-MB-231 cells. D) Specificity of F3-mediated internalization of F3-GFP-H6 protein. Internalization was

significantly reduced when lactoferrin was pre-incubated in MDA-MB-231 cells. All data are presented as mean ± SEM (n=3).

First, we were interested in confirming the specificity of the F3-nucleolin interaction in the modular constructions generated here. The specific F3-nucleolin binding had been already demonstrated in other systems,[29,34,35] including fusion proteins,[33] but we were interested to obtain a full confirmation that such interaction would be maintained in a complex modular protein such as F3-GFP-H6. Since lactoferrin is a natural ligand of nucleolin,[39] we selected this glycoprotein to challenge the binding of F3-GFP-H6 to MDA-MB-231 cells. Interestingly, when added in a 1:3 or 1:10 molar excess to F3-GFP-H6-exposed cell cultures (1 μM), LTF significantly inhibits the internalization of the fusion protein in a dose-dependent manner (Figure 2D, p=0.002 and p=0.001 for 1:3 and 1:10, respectively). This finding confirmed the specificity of the construct for nucleolin on the cell surface, and the potential of the ligand F3 as a protein tool for precision molecular delivery in form of complex multidomain modular protein. To take it a step further, we focused on the engineering of the modular protein to promote its self-assembling as protein-only nanoparticles. Enhancing the cationic character of the amino-terminal segment of H6-tagged proteins promotes their self-assembling as toroid nanoparticles,[40] in which the overhanging H6 tails strongly contribute through divalent cation coordination.[41] The combined occurrence of a cationic N-terminal region plus a histidine-rich C-terminal peptide represents a well-known platform to promote protein oligomerization, irrespective of the precise amino acid sequence of the core region.[42] Self-assembling of such modular proteins is promoted by electrostatic interactions[42] and stabilized by cross-coordination of overhanging histidine-rich tails with divalent cations.[41,43] The combination of these two types of interactions results in nanoparticles with a structural organization compatible with toroidal forms,[41,44] and that are

stable upon in vivo administration even after dilution in the bloodstream.[45] A controlled oligomerization of F3-GFP-H6 would offer multiple F3 display, optimal nanoscale size and a cooperative virus-like binding to the cell receptor [46] for enhanced penetration and precise whole-body biodistribution.[47] For that, we constructed a longer fusion F3-RK-GFP-H6 by the incorporation of the policationic RKRKRKRK motif (Figure 3A). The protein was produced in a stable form as a single species and successfully assembled as 16 and 12 mm nanoparticles (Figure 3A and 3B), that were fluorescent both in carbonate buffer (C) and carbonate with salt buffer (CS). Oligomerization of F3-GFP-H6 by the incorporation of the RK domain resulted in a dramatic enhancement of the cellular uptake (Figure 3C), that as in the case of the simpler protein construct was still nucleolin-dependent, since it was clearly inhibited by lactoferrin (Figure 3D, p= 0.013) in the version dialyzed against carbonate with salt buffer (CS). Cellular uptake and intracellular localization of the F3-RK-GFP-H6 construct was further confirmed by confocal imaging (Supplementary Figure 3). Such internalization and specificity was not observed in the version in carbonate buffer (C), probably due to an enhanced but differential building-blocks compactability and disposition when oligomerized in low ionic strength environment, as it can be observed in the mean hydrodynamic sizes (Figure 3A). Only a well oriented self-assembly will allow efficient and specific peptide-mediated internalization. This confirmed that nanoparticle formation through self-assembling is a powerful strategy to improve the molecular delivery properties of F3.

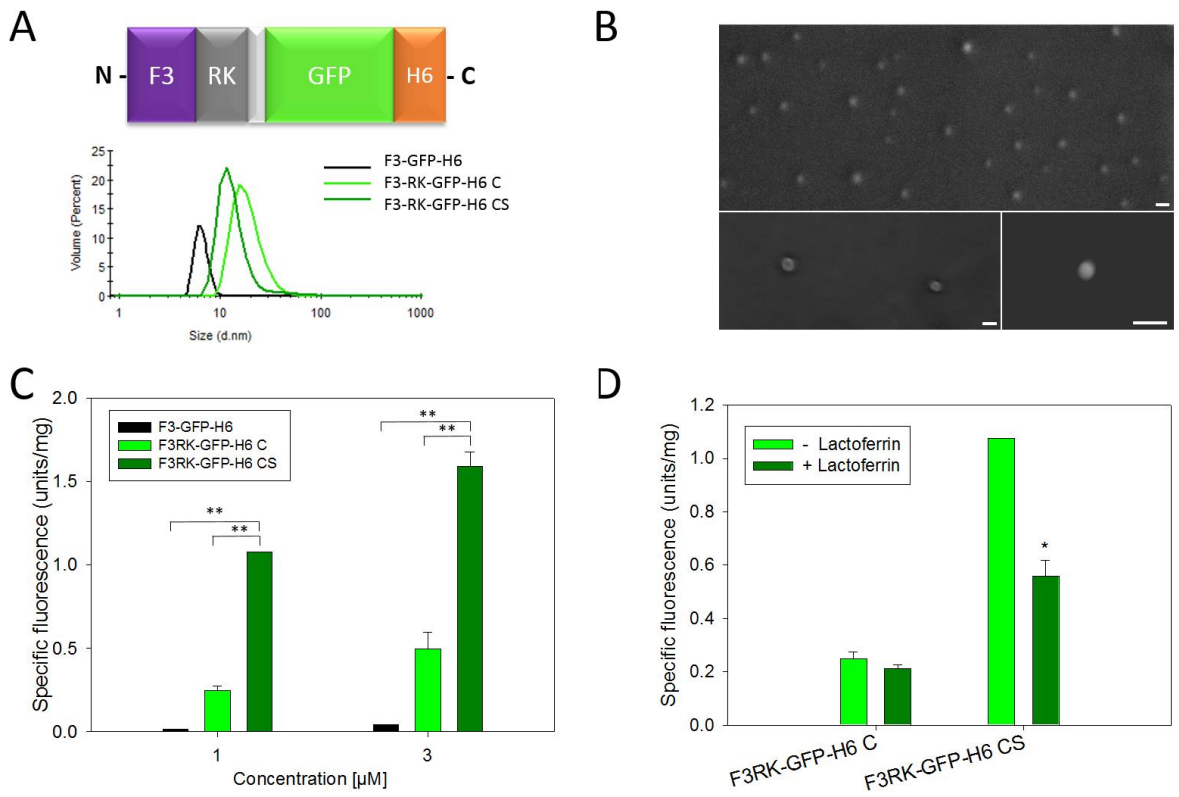

Figure 3. Physicochemical and functional characterization of F3-RK-GFP-H6 modular protein. A) Modular organization of the rationally designed F3-RK-GFP-H6 (top). In light grey is represented the linker sequence (GGSSRSS) added for conformational reasons. Dynamic light scattering (bottom) comparing parental F3-GFP-H6 and the newly designed F3-RK-GFP-H6 nanoparticle in carbonate (C) and carbonate with salt (CS) buffer. B) Field Emission Scanning Electron Microscopy of newly produced F3RK-GFP-H6 (CS) nanoparticles. Bars size: 30 nm. C) Internalization of F3-empowered modular proteins in MDA-MB-231 cells at 1 and 3 µM after 1 h incubation. Significant differences between relevant data are indicated with asterisks. D) Specific internalization of F3-RK-GFP-H6 nanoparticles, through the addition of LTF at 1:3 ratio (1 µM protein: 3 µM competitor). All data are presented as mean ± SEM (n=3).

At this stage, we decided to go forward and test if the developed platform could be suitable to generate nucleolin-targeted antitumoral drugs with nanostructure. For that, we replaced the irrelevant GFP domain by PE24, the exotoxin A of *Pseudomonas aeruginosa* that is under pre-clinical development as antitumoral drug.[12,48] Exotoxin A is a highly cytotoxic ribosome inactivating protein (RIP), described to inhibit the eukaryotic elongation factor 2 (EF-2) through ADP-ribosylation. When located in the cytoplasm of the host cell, exotoxin A inactivates EF-2, causing irreversible protein synthesis inhibition and cell death.[49] PE24, targeted to the tumor marker CXCR4, has recently shown to be an excellent cytotoxic drug for the treatment of colorectal cancer.[50] Over these premises, F3-RK-PE24-H6 was designed and produced as a single protein species (Figure 4A), that as in the case of the simpler version self-assembled as 20 nm-nanoparticles (Figure 4A and 4B), fully stable at high dilutions until at least 0.05 mg/mL, the detection limit of the DLS analyzer (data not shown). These materials caused dose-dependent MDA-MB-231 cell death (Figure 4C), which was inhibited by the addition of the competitor LTF. Addition of LFT rescued cell viability and therefore confirmed the specificity of the cell-entry mechanism (Figure 4D, p= 0.038).

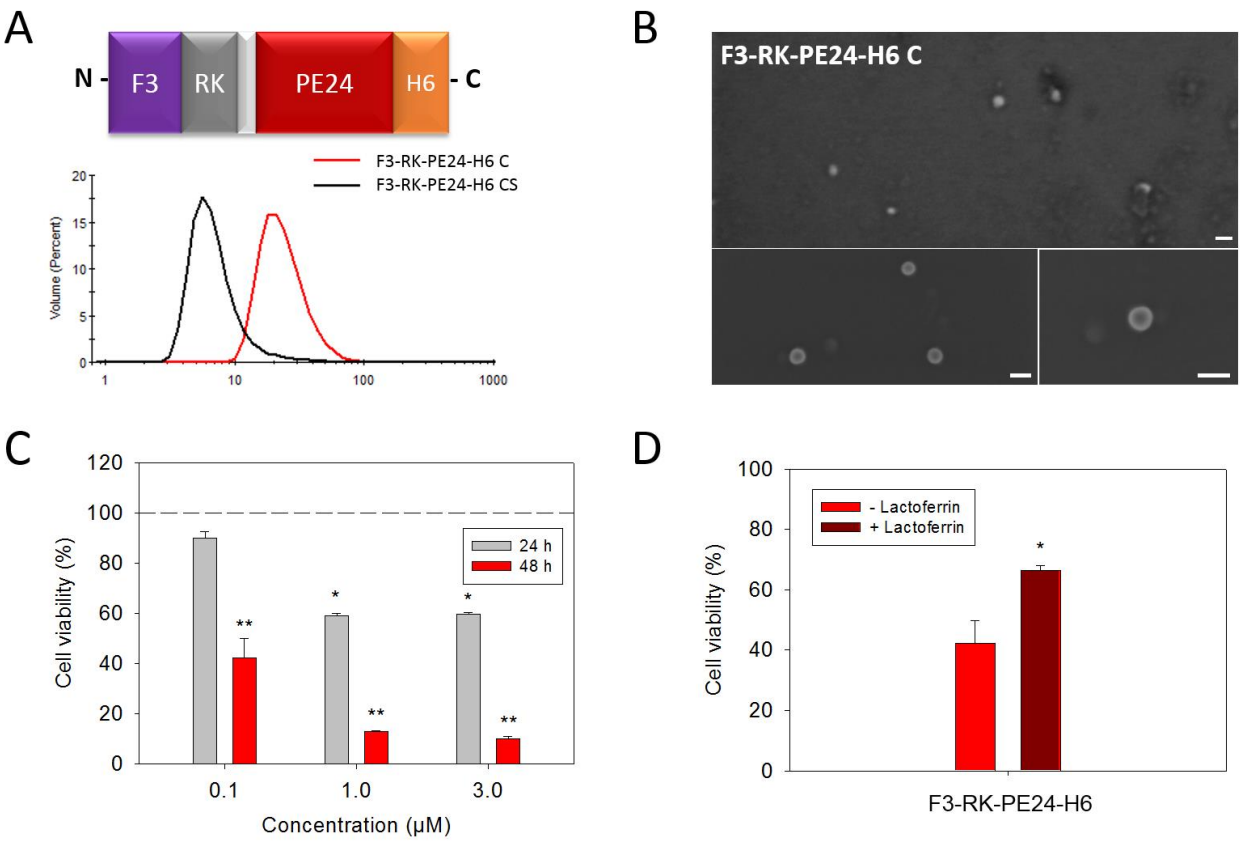

Figure 4. Physicochemical and functional characterization of the intrinsically cytotoxic F3-RK-PE24-H6. A) Modular organization of the rationally designed F3RK-PE24-H6 (top). The cytotoxic domain PE24 corresponds to the exotoxin A from *Pseudomonas aeruginosa*. Dynamic light scattering (bottom) of F3-RK-PE24-H6 modular protein dialyzed in carbonate (C) and carbonate with salt (CS) buffer. B) Field Emission Scanning Electron Microscopy of newly produced cytotoxic F3RK-PE24-H6 (C) nanoparticles. Bars size: 30 nm C) Cytotoxicity induced by F3-RK-PE24-H6 nanoparticles in MDA-MB-231 cells after the exposure to 0.1, 1 and 3 μM for 24 and 48 h. Statistical comparisons are made against the non-treated control cells. D) Reversion of cellular death (at 0.1 μM, 48 h) by the addition of the nucleolin competitor lactoferrin (ratio 1:3). All data are presented as mean ± SEM (n=3).

4. Conclusions

In this work we explore the use of receptor targeted peptide constructs with the idea of targeting specifically the CSC subpopulation within breast tumors. Screening of peptide ligands on CSC and non-CSC enriched cell cultures, revealed that F3 and pwt14 or p17, binding nucleolin and CXCR1 respectively, act as good ligands to facilitate the entry inside CSC in breast cancer cell cultures. Incorporation of these peptide sequences in larger peptide constructs increased the cell internalization and revealed that F3 outstand other ligands as a targeting moiety. Based on these results, we built a second-generation protein nanoparticles incorporating the policationic RKRKRKRK motif and the PE24 therapeutic domain. Indeed, F3-RK-PE24-H6, inhibited the growth of MDA-MB-231 breast cancer cell in a dose-dependent and receptor-specific manner, opening new avenues for future, nanoparticle-based CSC-targeted treatments.

ASSOCIATED CONTENT

Supporting Information. Peptide labeling strategy, MALDI characterization of recombinant proteins and confocal imaging of the cell internalization of F3RK-GFP-H6 is shown in a single PDF file.

AUTHOR INFORMATION

Corresponding Author

* AV antoni.villaverde@uab.cat; IA ibane.abasolo@vhir.org

Present Addresses

†RB-F: Department of Ruminant Production, Institut de Recerca i Tecnologia Agroalimentàries (IRTA), Caldes de Montbui, 08140, Barcelona, **Spain**.

Author Contributions

MP and LS-G produced, purified and tested the protein constructs with the aid of NS. JS, RB-F, PG and PC conducted the peptide internalization assays and contributed also the testing of protein constructs. DP, JJJ synthesized, fluorochrome label and purified the peptide ligands, previously selected by MR, IA and EV. The manuscript was written through contributions of all authors. Initial writing was conducted mainly by AV and IAO, with key contributions by MP, LS-G and MR. Funding and technical resources to complete the experiments were provided by MR, SS, AV, IAO and EV. All authors contributed to the experimental design and discussion of the results, including a careful revision and approval of the final manuscript.

‡These authors contributed equally

Funding Sources

This study has been supported by La Fundació Marató TV3 (TV32013-133930-1-2) and CIBER-BBN (NanoCanTri) to EV, MR and IA, and partially by ISCIII (PI15/00272, PI17/02242 and PI18/00871 co-founded by Fondo Europeo de Desarrollo Regional (FEDER), to EV, SS and IA respectively), Agencia Estatal de Investigación (AEI) and FEDER (BIO2016-76063-R to AV and SAF2014-60138-R to MR), AGAUR (2017SGR-229 to AV and 2017-SGR-1439 to MR) and CIBER-BBN (VENOM4CANCER granted to AV). LSG was supported by predoctoral fellowship from AGAUR (2018FI_B2_00051). JSF was supported by an AECC post-doctoral fellowship (AIO14142112SERA). AV received an ICREA ACADEMIA award.

ACKNOWLEDGMENT

Protein production and DLS have been partially performed by the ICTS "NANBIOSIS", more specifically by the Protein Production Platform of CIBER-BBN/IBB (http://www.nanbiosis.es/unit/u1-protein-production-platform-ppp/) and the Biomaterial Processing and Nanostructuring Unit (http://www.nanbiosis.es/portfolio/u6-biomaterial-processing-and-nanostructuring-unit/), respectively. Cancer stem cell internalization assays were performed at the ICTS "NANBIOSIS", specifically by U20/FVPR (http://www.nanbiosis.es/portfolio/u20-in-vivo-experimental-platform/). Peptide syntheses were performed ant the ICTS "NANBIOSIS", specifically at the unit of synthesis of peptides (U3/IQAC-CSIC).

ABBREVIATIONS

BSA, bovine serum albumin; C, carbonate buffer; CF, carboxyfluorescein; CS, carbonate buffer with salt; CSC, cancer stem cells; DCM, dichloromethane; DIC, diisopropylcarbodiimide; DIEA, diisopropylethylamine; DMAP, dimethylaminopyridine; DMF, dimethylformamide; epidermal growth factor; ER, estrogen receptor; GFP, green fluorescent protein; FGFb, basic fibroblast grothw factor; IPTG, isopropyl β-d-1-thiogalactopyranoside; PE24, exotoxin A of *Pseudomonas aeruginosa;* PgR, progesterone receptor; TFA, diisopropylethylamine; TNBC, triple negative breast cancer;

REFERENCES

(1) Bray F., Ferlay J., Soerjomataram I., Siegel R.L., Torre L.A., J. A. Global Cancer Statistics 2018: GLof Incidence and Mortality World in 185 Countries. *CA Cancer J ClinAnticancer Res.* **2018**. https://doi.org/10.3322/caac.21492.

(2) Foulkes, W. D.; Smith, I. E.; Reis-Filho, J. S. Triple-Negative Breast Cancer. *The New England journal of medicine*. 2010, pp 1938–1948. https://doi.org/10.1056/NEJMra1001389.

(3) Sledge, G. W.; Neuberg, D.; Bernardo, P.; Ingle, J. N.; Martino, S.; Rowinsky, E. K.; Wood, W. C. Phase III Trial of Doxorubicin, Paclitaxel, and the Combination of Doxorubicin and Paclitaxel as Front-Line Chemotherapy for Metastatic Breast Cancer: An Intergroup Trial (E1193). *J. Clin. Oncol.* **2003**, *21* (4), 588–592. https://doi.org/10.1200/JCO.2003.08.013.

(4) Arnedos, M.; Bihan, C.; Delaloge, S.; Andre, F. Triple-Negative Breast Cancer: Are We Making Headway at Least? *Therapeutic Advances in Medical Oncology*. 2012, pp 195–210. https://doi.org/10.1177/1758834012444711.

(5) Moreno-Aspitia, A.; Perez, E. A. Treatment Options for Breast Cancer Resistant to Anthracycline and Taxane. *Mayo Clin. Proc.* **2009**, *84* (6), 533–545. https://doi.org/10.1016/S0025-6196(11)60585-5.

(6) Margaryan, N. V.; Jenkins, H. H.; Salkeni, M. A.; Smolkin, M. B.; Coad, J. A.; Wen, S.; Seftor, E. A.; Seftor, R. E. B.; Hendrix, M. J. C. The Stem Cell Phenotype of Aggressive Breast Cancer Cells. *Cancers (Basel).* **2019**, *11* (3). https://doi.org/10.3390/cancers11030340.

(7) Dey, P.; Rathod, M.; De, A. Targeting Stem Cells in the Realm of Drug-Resistant Breast Cancer. *Breast cancer (Dove Med. Press.* **2019**, *11*, 115–135. https://doi.org/10.2147/BCTT.S189224.

(8) Gener, P.; Rafael, D. F. de S.; Fernández, Y.; Ortega, J. S.; Arango, D.; Abasolo, I.; Videira, M.; Schwartz, S. Cancer Stem Cells and Personalized Cancer Nanomedicine. *Nanomedicine* **2016**, *11* (3), 307–320. https://doi.org/10.2217/nnm.15.200.

(9) Jain, R. K.; Stylianopoulos, T. Delivering Nanomedicine to Solid Tumors. *Nature Reviews Clinical Oncology*. November 2010, pp 653–664. https://doi.org/10.1038/nrclinonc.2010.139.

(10) Shi, J.; Kantoff, P. W.; Wooster, R.; Farokhzad, O. C. Cancer Nanomedicine: Progress, Challenges and Opportunities. *Nature Reviews Cancer*. Nature Publishing Group January 1, 2017, pp 20–37. https://doi.org/10.1038/nrc.2016.108.

(11) Shen, J.; Wolfram, J.; Ferrari, M.; Shen, H. Taking the Vehicle out of Drug Delivery. *Materials Today*. Elsevier B.V. April 1, 2017, pp 95–97. https://doi.org/10.1016/j.mattod.2017.01.013.

(12) Serna, N.; Sánchez-García, L.; Unzueta, U.; Díaz, R.; Vázquez, E.; Mangues, R.; Villaverde, A. Protein-Based Therapeutic Killing for Cancer Therapies. *Trends in Biotechnology*. Elsevier Ltd March 1, 2018, pp 318–335. https://doi.org/10.1016/j.tibtech.2017.11.007.

(13) Casanova, I.; Unzueta, U.; Arroyo-Solera, I.; Céspedes, M. V.; Villaverde, A.; Mangues, R.; Vazquez, E. Protein-Driven Nanomedicines in Oncotherapy. *Current Opinion in*

Pharmacology. Elsevier Ltd August 1, 2019, pp 1–7. https://doi.org/10.1016/j.coph.2018.12.004.

(14) Fonseca, N. A.; Rodrigues, A. S.; Rodrigues-Santos, P.; Alves, V.; Gregório, A. C.; Valério-Fernandes, Â.; Gomes-da-Silva, L. C.; Rosa, M. S.; Moura, V.; Ramalho-Santos, J.; Simões S.; Moreira J.N. Nucleolin Overexpression in Breast Cancer Cell Sub-Populations with Different Stem-like Phenotype Enables Targeted Intracellular Delivery of Synergistic Drug Combination. *Biomaterials* **2015**, *69*, 76–88. https://doi.org/10.1016/j.biomaterials.2015.08.007.

(15) D'Avino, C.; Palmieri, D.; Braddom, A.; Zanesi, N.; James, C.; Cole, S.; Salvatore, F.; Croce, C. M.; De Lorenzo, C. A Novel Fully Human Anti-NCL ImmunoRNase for Triple-Negative Breast Cancer Therapy. *Oncotarget* **2016**, *7* (52), 87016–87030. https://doi.org/10.18632/oncotarget.13522.

(16) Brandolini, L.; Cristiano, L.; Fidoamore, A.; Pizzol, M. De; Giacomo, E. Di; Florio, T. M.; Confalone, G.; Galante, A.; Cinque, B.; Benedetti, E.; Ruffini P.A.; Cifone M.G.; Giordano A.; Alecci M.; Allegretti M.; Cimini A. Targeting CXCR1 on Breast Cancer Stem Cells: Signaling Pathways and Clinical Application Modelling. *Oncotarget* **2015**, *6* (41), 43375–43394. https://doi.org/10.18632/oncotarget.6234.

(17) Xue, M. Q.; Liu, J.; Sang, J. F.; Su, L.; Yao, Y. Z. Expression Characteristic of CXCR1 in Different Breast Tissues and the Relevance between Its Expression and Efficacy of Neoadjuvant Chemotherapy in Breast Cancer. *Oncotarget* **2017**, *8* (30), 48930–48937. https://doi.org/10.18632/oncotarget.16893.

(18) Yoshimura, T.; Oppenheim, J. J. Chemokine-like Receptor 1 (CMKLR1) and Chemokine

(C-C Motif) Receptor-like 2 (CCRL2); Two Multifunctional Receptors with Unusual Properties. *Experimental Cell Research*. Academic Press Inc. 2011, pp 674–684. https://doi.org/10.1016/j.yexcr.2010.10.023.

(19) Snyder, E. L.; Bailey, D.; Shipitsin, M.; Polyak, K.; Loda, M. Identification of CD44v6 /CD24 Breast Carcinoma Cells in Primary Human Tumors by Quantum Dot-Conjugated Antibodies. *Lab. Investig.* **2009**, *89* (8), 857–866. https://doi.org/10.1038/labinvest.2009.54.

(20) Krishnamachary, B.; Penet, M. F.; Nimmagadda, S.; Mironchik, Y.; Raman, V.; Solaiyappan, M.; Semenza, G. L.; Pomper, M. G.; Bhujwalla, Z. M. Hypoxia Regulates CD44 and Its Variant Isoforms through HIF-1α in Triple Negative Breast Cancer. *PLoS One* **2012**, *7* (8). https://doi.org/10.1371/journal.pone.0044078.

(21) Charafe-Jauffret, E.; Ginestier, C.; Iovino, F.; Wicinski, J.; Cervera, N.; Finetti, P.; Hur, M. H.; Diebel, M. E.; Monville, F.; Dutcher, J.; Brown M.; Viens P.; Xerri L.; Bertucci F.; Stassi G.; Dontu G.; Birnbaum D.; Wicha M.S. Breast Cancer Cell Lines Contain Functional Cancer Stem Sells with Metastatic Capacity and a Distinct Molecular Signature. *Cancer Res.* **2009**, *69* (4), 1302–1313. https://doi.org/10.1158/0008-5472.CAN-08-2741.

(22) Gener, P.; Rafael, D.; Seras-Franzoso, J.; Perez, A.; Pindado, L. A.; Casas, G.; Arango, D.; Fernández, Y.; Díaz-Riascos, Z. V; Abasolo, I.; Schwartz S.Jr. Pivotal Role of AKT2 during Dynamic Phenotypic Change of Breast Cancer Stem Cells. *Cancers (Basel).* **2019**, *11* (8). https://doi.org/10.3390/cancers11081058.

(23) Holliday, D. L.; Speirs, V. Choosing the Right Cell Line for Breast Cancer Research.

Breast Cancer Research. August 12, 2011. https://doi.org/10.1186/bcr2889.

(24) Matzke-Ogi, A.; Jannasch, K.; Shatirishvili, M.; Fuchs, B.; Chiblak, S.; Morton, J.; Tawk, B.; Lindner, T.; Sansom, O.; Alves, F.; Warth A.; Schwager C.; Mier W.; Kleeff J.; Ponta H.; Abdollahi A.; Orian-Rousseau V. Inhibition of Tumor Growth and Metastasis in Pancreatic Cancer Models by Interference with CD44v6 Signaling. *Gastroenterology* **2016**, *150* (2), 513-525.e10. https://doi.org/10.1053/j.gastro.2015.10.020.

(25) Ginestier, C.; Liu, S.; Diebel, M. E.; Korkaya, H.; Luo, M.; Brown, M.; Wicinski, J.; Cabaud, O.; Charafe-Jauffret, E.; Birnbaum, D.; Guan J.L.; Dontu G.; Wicha M.S. CXCR1 Blockade Selectively Targets Human Breast Cancer Stem Cells in Vitro and in Xenografts. *J. Clin. Invest.* **2010**, *120* (2), 485–497. https://doi.org/10.1172/JCI39397.

(26) Jiang, S. J.; Liou, J. W.; Chang, C. C.; Chung, Y.; Lin, L. F.; Hsu, H. J. Peptides Derived from CXCL8 Based on in Silico Analysis Inhibit CXCL8 Interactions with Its Receptor CXCR1. *Sci. Rep.* **2015**, *5*. https://doi.org/10.1038/srep18638.

(27) Li, L.; Huang, C.; Zhang, X.; Wang, J.; Ma, P.; Liu, Y.; Xiao, T.; Zabel, B. A.; Zhang, J. V. Chemerin-Derived Peptide C-20 Suppressed Gonadal Steroidogenesis. *Am. J. Reprod. Immunol.* **2014**, *71* (3), 265–277. https://doi.org/10.1111/aji.12164.

(28) Doyle, J. R.; Krishnaji, S. T.; Zhu, G.; Xu, Z.-Z.; Heller, D.; Ji, R.-R.; Levy, B. D.; Kumar, K.; Kopin, A. S. Development of a Membrane-Anchored Chemerin Receptor Agonist as a Novel Modulator of Allergic Airway Inflammation and Neuropathic Pain. *J. Biol. Chem.* **2014**, *289* (19), 13385–13396. https://doi.org/10.1074/jbc.M113.522680.

(29) Lam, P. Y. H.; Hillyar, C. R. T.; Able, S.; Vallis, K. A. Synthesis and Evaluation of an

18F-Labeled Derivative of F3 for Targeting Surface-Expressed Nucleolin in Cancer and Tumor Endothelial Cells. *J. Label. Compd. Radiopharm.* **2016**, 492–499. https://doi.org/10.1002/jlcr.3439.

(30) Cornelissen, B.; Waller, A.; Target, C.; Kersemans, V.; Smart, S.; Vallis, K. A. 111In-BnDTPA-F3: An Auger Electron-Emitting Radiotherapeutic Agent That Targets Nucleolin. *EJNMMI Res.* **2012**, *2* (1), 1–11. https://doi.org/10.1186/2191-219X-2-9.

(31) Giagulli, C.; Magiera, A. K.; Bugatti, A.; Caccuri, F.; Marsico, S.; Rusnati, M.; Vermi, W.; Fiorentini, S.; Caruso, A. HIV-1 Matrix Protein P17 Binds to the IL-8 Receptor CXCR1 and Shows IL-8-like Chemokine Activity on Monocytes through Rho/ROCK Activation. *Blood* **2012**, *119* (10), 2274–2283. https://doi.org/10.1182/blood-2011-06-364083.

(32) Caccuri, F.; Marsico, S.; Fiorentini, S.; Caruso, A.; Giagulli, C. HIV-1 Matrix Protein P17 and Its Receptors. *Curr. Drug Targets* **2016**, *17* (1), 23–32.

(33) Ham, S. H.; Min, K. A.; Shin, M. C. Molecular Tumor Targeting of Gelonin by Fusion with F3 Peptide. *Acta Pharmacol. Sin.* **2017**, *38* (6), 897–906. https://doi.org/10.1038/aps.2017.20.

(34) Christian, S.; Pilch, J.; Akerman, M. E.; Porkka, K.; Laakkonen, P.; Ruoslahti, E. Nucleolin Expressed at the Cell Surface Is a Marker of Endothelial Cells in Angiogenic Blood Vessels. *J. Cell Biol.* **2003**, *163* (4), 871–878. https://doi.org/10.1083/jcb.200304132.

(35) Romano, S.; Moura, V.; Simões, S.; Moreira, J. N.; Gonçalves, J. Anticancer Activity and

Antibody-Dependent Cell-Mediated Cytotoxicity of Novel Anti-Nucleolin Antibodies. *Sci. Rep.* **2018**, *8* (1). https://doi.org/10.1038/s41598-018-25816-8.

(36) Romano, S.; Fonseca, N.; Simões, S.; Gonçalves, J.; Moreira, J. N. Nucleolin-Based Targeting Strategies for Cancer Therapy: From Targeted Drug Delivery to Cytotoxic Ligands. *Drug Discovery Today*. Elsevier Ltd 2019. https://doi.org/10.1016/j.drudis.2019.06.018.

(37) Balça-Silva, J.; do Carmo, A.; Tão, H.; Rebelo, O.; Barbosa, M.; Moura-Neto, V.; Sarmento-Ribeiro, A. B.; Lopes, M. C.; Moreira, J. N. Nucleolin Is Expressed in Patient-Derived Samples and Glioblastoma Cells, Enabling Improved Intracellular Drug Delivery and Cytotoxicity. *Exp. Cell Res.* **2018**, *370* (1), 68–77. https://doi.org/10.1016/j.yexcr.2018.06.005.

(38) Ferrer-Miralles, N.; Corchero, J. L.; Kumar, P.; Cedano, J. A.; Gupta, K. C.; Villaverde, A.; Vazquez, E. Biological Activities of Histidine-Rich Peptides; Merging Biotechnology and Nanomedicine. *Microb. Cell Fact.* **2011**, *10*, 101. https://doi.org/10.1186/1475-2859-10-101.

(39) Legrand, D.; Vigié, K.; Said, E. A.; Elass, E.; Masson, M.; Slomianny, M.-C.; Carpentier, M.; Briand, J.-P.; Mazurier, J.; Hovanessian, A. G. Surface Nucleolin Participates in Both the Binding and Endocytosis of Lactoferrin in Target Cells. *Eur. J. Biochem.* **2004**, *271* (2), 303–317. https://doi.org/10.1046/j.1432-1033.2003.03929.x.

(40) Serna, N.; Céspedes, M. V.; Saccardo, P.; Xu, Z.; Unzueta, U.; Álamo, P.; Pesarrodona, M.; Sánchez-Chardi, A.; Roldán, M.; Mangues, R.; et al. Rational Engineering of Single-Chain Polypeptides into Protein-Only, BBB-Targeted Nanoparticles. *Nanomedicine*

Nanotechnology, Biol. Med. **2016**, *12* (5), 1241–1251. https://doi.org/10.1016/j.nano.2016.01.004.

(41) López-Laguna, H.; Unzueta, U.; Conchillo-Solé, O.; Sánchez-Chardi, A.; Pesarrodona, M.; Cano-Garrido, O.; Voltà, E.; Sánchez-García, L.; Serna, N.; Saccardo, P.; Mangues R.; Villaverde A.; Vázquez E. Assembly of Histidine-Rich Protein Materials Controlled through Divalent Cations. *Acta Biomater.* **2019**, *83*, 257–264. https://doi.org/10.1016/j.actbio.2018.10.030.

(42) Unzueta, U.; Ferrer-Miralles, N.; Cedano, J.; Zikung, X.; Pesarrodona, M.; Saccardo, P.; García-Fruitós, E.; Domingo-Espín, J.; Kumar, P.; Gupta, K. C.; Mangues R.; Villaverde A.; Vazquez E. Non-Amyloidogenic Peptide Tags for the Regulatable Self-Assembling of Protein-Only Nanoparticles. *Biomaterials* **2012**, *33* (33), 8714–8722. https://doi.org/10.1016/j.biomaterials.2012.08.033.

(43) Voltà-Durán, E.; Cano-Garrido, O.; Serna, N.; López-Laguna, H.; Sánchez-García, L.; Pesarrodona, M.; Sánchez-Chardi, A.; Mangues, R.; Villaverde, A.; Vázquez, E.; Unzueta U. Controlling Self-Assembling and Tumor Cell-Targeting of Protein-Only Nanoparticles through Modular Protein Engineering. *Sci. China Mater.* **2019**. https://doi.org/10.1007/s40843-019-9582-9.

(44) Rueda, F.; Céspedes, M. V.; Conchillo-Solé, O.; Sánchez-Chardi, A.; Seras-Franzoso, J.; Cubarsi, R.; Gallardo, A.; Pesarrodona, M.; Ferrer-Miralles, N.; Daura, X.; Vázquez E.; García-Fruitós E.; Mangues R.; Unzueta U.; Villaverde A. Bottom-Up Instructive Quality Control in the Biofabrication of Smart Protein Materials. *Adv. Mater.* **2015**, *27* (47), 7816–7822. https://doi.org/10.1002/adma.201503676.

(45) Céspedes, M. V.; Unzueta, U.; Tatkiewicz, W.; Sánchez-Chardi, A.; Conchillo-Solé, O.; Álamo, P.; Xu, Z.; Casanova, I.; Corchero, J. L.; Pesarrodona, M.; Cedano J.; Daura X.; Ratera I.; Veciana J.; Ferrer-Miralles N.; Vazquez E.; Villaverde A.; Mangues R. In Vivo Architectonic Stability of Fully de Novo Designed Protein-Only Nanoparticles. *ACS Nano* **2014**. https://doi.org/10.1021/nn4055732.

(46) Unzueta, U.; Céspedes, M. V.; Vázquez, E.; Ferrer-Miralles, N.; Mangues, R.; Villaverde, A. Towards Protein-Based Viral Mimetics for Cancer Therapies. *Trends in Biotechnology*. Elsevier Ltd May 1, 2015, pp 253–258. https://doi.org/10.1016/j.tibtech.2015.02.007.

(47) López-Laguna, H.; Sala, R.; Sánchez, J. M.; Álamo, P.; Unzueta, U.; Sánchez-Chardi, A.; Serna, N.; Sánchez-García, L.; Voltà-Durán, E.; Mangues, R.; Villaverde A.; Vázquez E. Nanostructure Empowers Active Tumor Targeting in Ligand-Based Molecular Delivery. *Part. Part. Syst. Charact.* **2019**, 1900304. https://doi.org/10.1002/ppsc.201900304.

(48) Sanchez-Garcia, L.; Martín, L.; Mangues, R.; Ferrer-Miralles, N.; Vázquez, E.; Villaverde, A. Recombinant Pharmaceuticals from Microbial Cells: A 2015 Update. *Microb. Cell Fact.* **2016**, *15*, 33. https://doi.org/10.1186/s12934-016-0437-3.

(49) Michalska, M.; Wolf, P. Pseudomonas Exotoxin A: Optimized By1. Michalska M, Wolf P. Pseudomonas Exotoxin A: Optimized by Evolution for Effective Killing. *Front. Microbiol.* **2015**, *6* (SEP), 1–7. https://doi.org/10.3389/fmicb.2015.00963.

(50) Sánchez-García, L.; Serna, N.; Álamo, P.; Sala, R.; Céspedes, M. V.; Roldan, M.; Sánchez-Chardi, A.; Unzueta, U.; Casanova, I.; Mangues, R.; Vázquez E.; Villaverde A. Self-Assembling Toxin-Based Nanoparticles as Self-Delivered Antitumoral Drugs. *J. Control. Release* **2018**, *274*, 81–92. https://doi.org/10.1016/j.jconrel.2018.01.031.

TABLE OF CONTENTS GRAPHIC (at the actual size to be used, 8.25 x 4.45 cm)